ELSEVIER

Nuclear Physics A 586 (1995) 445–456

NUCLEAR PHYSICS A

Shell-model calculations for neutron-rich nuclei in the 0f1p shell

W.A. Richter [a], M.G. Van der Merwe [a], B.A. Brown [b]

[a] *Physics Department, University of Stellenbosch, Stellenbosch 7600, South Africa*

[b] *National Superconducting Cyclotron Laboratory and Department of Physics and Astronomy, Michigan State University, East Lansing, MI 48824, USA*

Received 4 August 1994; revised 22 November 1994

Abstract

A new two-body interaction recently derived for nuclei in the 0f1p shell by fitting two-body matrix elements to 494 energy levels in $A = 41$–66 nuclei, is used to investigate the neutron-rich nuclei in the vicinity of the doubly closed nuclide ^{48}Ca. This study is of fundamental interest in providing a test for the new effective interaction away from the stability line. Masses and binding energies are calculated for a variety of neutron-rich nuclei and compared with experimental data, where available. In addition level schemes for $^{50-52}$Ca, $^{51-52}$Sc and $^{51-52}$Ti have been calculated and are compared with available experimental data. In general a good correspondence between theory and experiment is found, but some systematic discrepancies are apparent.

1. Introduction

A new two-body interaction was recently derived for nuclei in a large part of the 0f1p shell ($A = 41$–66) by considering a truncated fp configuration space incorporating 1p1h excitations from the $f_{7/2}$ shell, i.e. $0f_{7/2}^{n}(1p_{3/2}0f_{5/2}1p_{1/2})^{m} + 0f_{7/2}^{n-1}(1p_{3/2}0f_{5/2}1p_{1/2})^{m+1}$ configurations, with m the minimum number of nucleons outside the filled or partially filled $f_{7/2}$ shell [1,2]. The final interaction, denoted by TBLC8, was obtained by fitting to a set of 494 level energies. Good agreement was obtained with experimental values for the observables calculated with the TBLC8 wave functions, i.e. energy levels and static electromagnetic moments [1].

In view of the good results obtained with our TBLC8 interaction, it is appropriate to investigate the applicability of the interaction for nuclei further away from the line of stability. Section 2 contains a brief review of the TBLC8 interaction. In Section 3 we calculate the masses of a number of neutron-rich nuclei with the TBLC8 interaction and

SSDI 0375-9474(94)00802-7

compare the results with experiment. The shell-model calculations have been carried out on a VAX computer at the National Superconducting Cyclotron Laboratory, University of Michigan State using the OXBASH code [3]. Predictions are also given for some nuclei which have not yet been observed. In Section 4 we consider the level structure of some of the $N = 30$–32 isotones in the vicinity of the doubly closed ^{48}Ca nucleus.

2. The TBLC8 two-body interaction

When fitting two-body matrix elements and single-particle energies in the fp-shell to an energy data set, a very large number of parameters have to be determined from the data set. The number of parameters can however be restricted by a method referred to as the linear combination (LC) method [4]. The least-squares fit problem is reformulated in terms of uncorrelated linear combinations of the one- and two-body matrix elements, or "orthogonal" parameters. The orthogonal parameters can be ordered according to their uncertainty and the well-determined parameters separated from the poorly determined ones. Some constraints are imposed on the least-squares fit so that most of the matrix elements are held fixed at values corresponding to some starting interaction, except for those that are well-determined by the data set.

It was found that in order to get a good reproduction of the single-particle energies (SPE) of ^{41}Ca as well as a good overall fit, the single-particle energies must also be mass dependent. A simple linear mass dependence of the form

$$\mathrm{SPE}(A) = \mathrm{SPE}(A=41) + \frac{A-41}{66-41}[\mathrm{SPE}(A=66) - \mathrm{SPE}(A=41)] \tag{1}$$

was used for each of the four single-particle energies ($0f_{7/2}$, $1p_{3/2}$, $0f_{5/2}$ and $1p_{1/2}$).

In addition a mass dependence of the two-body matrix elements of the form A^{-p} was also assumed. The optimum value used was determined to be $p = 0.50$. The renormalized TBME, after consideration of the assumed mass dependence, will therefore be of the form

$$\langle V\rangle(A) = \langle V\rangle(A/42)^{-0.50}. \tag{2}$$

The fp-shell interaction is in principle determined by 195 TBME and the 8 SPE parameters. Due to the model space truncation 20 two-body matrix elements are not determined, and a further 6 are extremely insensitive to the data set, and are set equal to a starting interaction. The number of parameters that could be varied was therefore reduced to 177 parameters. The 40 best-determined linear combinations out of this set of 177 parameters were allowed to vary, while the remaining ones were fixed at the TBME4 starting interaction, determined in previous preliminary work [1]. An r.m.s deviation between fitted and experimental energies of 193 keV has been achieved. An excellent reproduction of low-lying energy levels, and the magnetic dipole and electric quadrupole moments for the ground states as well as some excited states, is obtained with the new interaction [1].

3. Masses of neutron-rich nuclei

The measurement of nuclear masses is of fundamental importance for assessing the predictions of nuclear models for gross properties, e.g. ground-state binding energies, or detailed properties, e.g. level structure, pairing energy and Coulomb energy systematics, and decay properties. In this section masses on the neutron-rich side of the valley of β-stability calculated with our TBLC8 interaction are compared with the most recent available measurements consisting of values from Seifert et al. [5], based on measurements with a time-of-flight isochronous (TOFI) spectrometer, and values from the 1993 mass compilation of Audi and Wapstra [6]. The advantage of comparing with one set of experimental data like that of Seifert et al. is that general trends are less likely to be obscured as a result of systematic errors which may vary from one experiment to another.

The Coulomb displacement energies required in the shell-model calculations have been obtained from the energy differences of analogue states, one generally being a ground state. The Coulomb contributions of the states used in the fits to obtain the TBLC8 interaction have been obtained in this way, and are discussed in Ref. [1]. In cases where one partner is not known experimentally estimates have been made using extrapolations of linear least-squares fits to known displacement energies. Because we use a ^{40}Ca core, we compare calculated and experimental binding energies $B_{\rm rel}$ relative to ^{40}Ca, where $B_{\rm rel} = B - B(^{40}{\rm Ca})$ and B is the absolute binding energy. The shell-model binding energy relative to ^{40}Ca can be expressed as $B_{\rm rel}^{\rm SM} = B_{\rm int} - C$, where $B_{\rm int}$ is the interaction energy between the extra-core nucleons calculated in the isospin formalism with our TBLC8 interaction, and C is the Coulomb displacement energy, estimated as described above.

A comparison with the results Seifert et al. [5] for the mass defects Δ, is given in Table 1. The masses for three very neutron-rich nuclei not measured by Seifert et al. are taken from the compilation of Audi and Wapstra [6]. Several cases in the region of $N = 31$ to $N = 37$ are absent from Table 1, because the shell-model dimension exceeds about 3500 and calculations have not yet been carried out. We make here a few comments about the most recent data from Seifert et al. in comparison with the previous TOFI data of Tu et al. [7] The values from Tu et al. and Seifert et al. are generally quite close to each other for $N < 36$, the largest difference being for ^{54}Sc where the value of Tu et al. is less bound than the value of Seifert et al. by about 0.9 MeV. For the most neutron-rich isotopes of V, Cr, Mn and Fe ($N \geqslant 36$) there are systematic deviations between the two sets, the values from Tu et al. always being less bound. The largest deviations in this group occur for ^{59,60}V (with respective deviations of about 2 and 1.6 MeV. respectively), for ^{61,62}Cr (deviations of about 1.2 and 1.7 MeV. respectively), for ^{63,64}Mn (deviations of about 0.9 MeV) and for ^{66}Fe (deviation about 1.5 MeV).

The differences $\Delta^{\rm SM} - \Delta^{\rm exp}$ are shown in Fig. 1. A negative value for this quantity indicates that experiment is more bound than theory. The circles correspond to experimental data from the compilation of Audi and Wapstra [6] and the crosses to experimental data

Table 1
Binding energies and mass defects for neutron-rich isotopes. B_{rel} is the binding energy relative to ^{40}Ca and Δ is the mass defect, both in units of MeV. SM stands for shell model, C for the estimated Coulomb displacement energy relative to Ca. The experimental values are from Seifert et al. [5] (a) or from the mass compilation [6] (b). The spin values given are predicted by our calculations

A	Element	N	$2J$	B_{rel}^{SM}	C	Δ^{exp}	Ref.	Δ^{SM}	$\Delta^{SM} - \Delta^{exp}$
51	Ca	31	3	89.20		−36.3(0.4)	a	−35.26	−1.0(0.4)
52		32	0	94.03		−32.5(0.5)	b	−32.01	−0.5(0.5)
52	Sc	31	6	101.39	7.12	−40.38(0.23)	a	−40.16	−0.22(0.23)
53		32	7	106.75	7.10	−38.96(0.26)	a	−37.44	−1.52(0.26)
54		33	6	109.95	7.09	−34.4(0.5)	a	−32.58	−1.82(0.5)
55		34	7	114.88	7.08	−28.5(1.0)	b	−29.43	0.9(1.0)
54	Ti	32	0	122.10	14.38	−45.76(0.23)	a	−45.52	−0.24(0.23)
55		33	1	125.83	14.34	−41.81(0.24)	a	−41.17	−0.64(0.24)
56		34	0	132.34	14.30	−39.13(0.28)	a	−39.61	0.48(0.28)
57		35	5	134.18	14.25	−33.3(1.0)	b	−33.37	0.1(1.0)
59	V	36	7	153.49	21.79	−37.91(0.35)	a	−37.32	−0.59(0.35)
60		37	2	156.36	21.73	−33.1(0.6)	a	−32.13	−1.0(0.6)
58	Cr	34	0	160.28	29.60	−51.93(0.24)	a	−52.97	1.04(0.24)
60		36	0	170.30	29.39	−46.83(0.26)	a	−46.84	0.01(0.26)
61		37	5	172.86	29.29	−42.77(0.28)	a	−41.33	−1.44(0.28)
62		38	0	178.32	29.17	−41.2(0.4)	a	−38.72	−2.48(0.4)
62	Mn	37	4	187.54	37.24	−48.47(0.26)	a	−48.73	0.26(0.26)
63		38	7	192.64	37.08	−46.75(0.28)	a	−45.76	−0.99(0.28)
64		39	2	195.76	36.93	−43.10(0.35)	a	−40.80	−2.30(0.35)
65		40	7	199.71	36.80	−40.9(0.6)	a	−36.68	−4.2(0.6)
63	Fe	37	5	201.84	45.33	−55.49(0.27)	a	−55.73	0.24(0.27)
64		38	0	209.16	45.09	−55.08(0.28)	a	−54.98	−0.10(0.28)
65		39	5	212.43	44.90	−51.29(0.28)	a	−50.18	−1.11(0.28)
66		40	0	217.72	44.77	−50.32(0.35)	a	−47.30	−2.92(0.35)

from Seifert et al. [5]. The filled circles for $N \leqslant 30$ indicate the more stable nuclei originally included in the A = 41–66 least-squares fit for our TBCL8 interaction [1]. It is evident that the TBLC8 interaction gives a good account of the measured binding energies or masses, with the theoretical values generally within 1 MeV of the measured values. The largest discrepancy with the TBLC8 interaction occurs for ^{65}Mn, where the deviation is about 4 MeV. The spins of the nuclei predicted by our calculations are also indicated in Table 1.

In Ref. [7] Tu et al. compare the differences between the theoretically predicted masses of four microscopic–macroscopic models and the experimental mass (see Fig. 3 of Ref. [7]). The models are those of Möller–Nix [8], Tachibana [9], the semi-empirical shell model of Liran–Zeldes [10] and Jänecke–Masson's recalculation of the Garvey–Kelson mass relationships [11]. Tu et al. found large systematic deviations for ^{51}Ca and $^{52-54}$Sc where the binding energies are significantly underpredicted. In Fig. 1 and Table 1 we note the same tendency, but our deviations of about 1 MeV are slightly less than the average of the four models in each case. As in Refs. [7,5] we also find that good general agreement between experiment and theory is restored for he Ti isotopes. This appears to support the suggestion of localized regions of enhanced binding for the

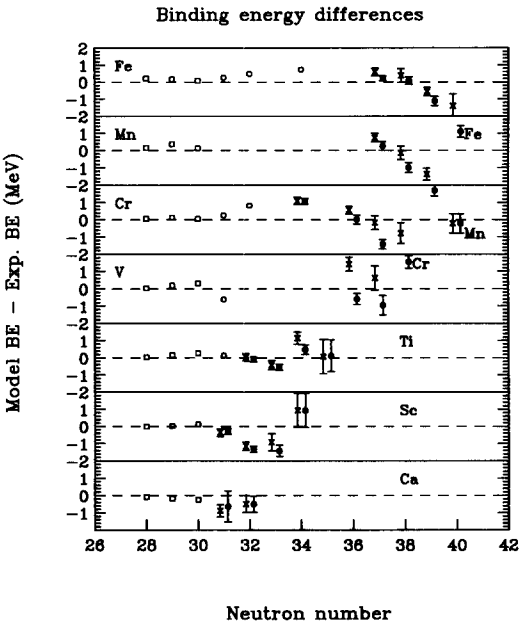

Fig. 1. $\Delta^{SM} - \Delta^{exp}$ versus neutron number N for neutron-rich nuclei. The crosses correspond to experimental masses from Seifert et al. [5] and the circles to compilation values from Ref. [6], where the filled circles indicate isotopes which were in the original least-squares fit of the TBLC8 interaction. Error bars are shown when they are larger than 0.4 MeV, and the values for a given isotope are connected by lines.

Ca and Sc isotopes [7,5]. It is also found that the binding of the most neutron-rich isotopes tend to be overpredicted by most of the four models, whereas our microscopic calculations tend to underpredict the binding of these isotopes by smaller amounts.

In Fig. 1 it can also be seen that there appears to be a systematic pattern for the three isotopes above V, which can be more readily seen for Fe and Cr where the data is more complete. A fairly smooth positive deviation is followed by a dramatic negative dive for the most neutron-rich species. In the case of the data from Tu et al. the deviation for the most neutron-rich nuclei is generally smaller than for the data from Seifert et al., implying less binding. When the $1p_{3/2}$ subshell is primarily being filled ($N = 29$ to 32), a very good reproduction of the experimental masses is observed, and when the $0f_{5/2}$ subshell is primarily being filled ($N = 33$ to 38), the shell model overpredicts the binding energy, which reaches a maximum at about the middle of the subshell. But when the $1p_{1/2}$ subshell is primarily being filled ($N = 39$ to 40) there is an increasing underprediction with N. The systematic deviations seem to indicate that the problem may lie with the description of the single-particle energies, or may indicate the presence of the $0g_{9/2}$ intruder orbital. The rather large positive deviation (1.4 MeV) found by Tu et al. for ^{59}V becomes a small negative deviation with the data of Seifert et al. It has been suggested in Ref. [7] that the presence of an unknown isomer may have affected the measurement for ^{59}V.

In some cases the calculations can be carried out for the full 0f1p model space,

employing the FPD6 interaction of Ref. [4]. In the full space the dimensions of the shell-model states increase rapidly with A and calculations can usually be carried out up to about mass 52 for the Ca isotopes. As the 0f1p shell is progressively filled it becomes again possible to carry out full-space calculations for some nuclei with masses larger than $A = 60$, e.g. ^{62}Cr. For masses near $A = 50$ the full-space calculation generally does somewhat better than the calculation in the FPV model space, e.g. for ^{51}Ca the calculated mass defects are -35.56 and -35.26 MeV for FPD6 and TBLC8, respectively, compared to the experimental value of $-36.3(0.4)$ MeV [5] and for ^{52}Ca the same quantities are -32.82 and -32.01 MeV for FPD6 and TBLC8, respectively, compared to $-32.5(0.5)$ MeV [6] for experiment. However, for the region around $A = 62$–66 where the full-space calculations are again possible, the theory becomes 10–20 MeV underbound compared to experiment. This is perhaps not surprising because the FPD6 interaction was only determined from energy data in the lower part of the 0f1p shell ($A = 41$–49).

We have also calculated a number of masses of neutron-rich nuclei for which no experimental information is available as yet. The predicted binding energies and mass defects are given in Table 2.

4. Level structure of the $N = 30$–32 isotones

Previous theoretical work in this region mainly concentrated on the use of a closed $0f_{7/2}$ neutron shell [12,13]. However, Huck et al. [14] included 1p1h jumps from the $0f_{7/2}$ subshell to the $1p_{3/2}$, $0f_{5/2}$ and $1p_{1/2}$ subshells. They investigated the isotopes ^{52}K, ^{52}Ca and ^{52}Sc by using the realistic Kuo–Brown interaction with a few monopole changes [15]. Their calculations showed that the structure of these nuclei can be described by the dominant configurations $0f_{7/2}^{12-n}r^n$ ($n = 4$, 3 and 2 respectively and $r=(1p_{3/2}0f_{5/2}1p_{1/2})$) and those reached through 1p1h jumps, $0f_{7/2}^{11-n}r^{n+1}$. This is the same model space used to obtain the TBLC8 interaction. The modified Kuo–Brown interaction also reproduced the relative energy levels reasonably well.

The experimental spectra for the low-lying normal-parity states are compared with those of the TBLC8 interaction in Figs. 2–8. The experimental information on spectroscopic quantities in this region is in general very limited. The data used for a comparison with the theoretical results obtained with the TBLC8 interaction were obtained from the Nuclear Data Sheets compilations (see Figs. 2–8), the Table of Isotopes of Lederer and Shirley [16], and from the study of the $A = 52$ isotopes by Huck et al. [14].

4.1. The N=30 isotones

^{50}Ca: The calculation gives an excitation energy of the first 2^+ state of 1.12 MeV compared to the experimental value of 1.026 MeV. The experimental level spectrum suggests that there is a large gap to the second excited state as predicted by the TBLC8 interaction.

Table 2
Predicted spins, binding energies and mass defects for neutron-rich nuclei. B_{rel} is the binding energy relative to ^{40}Ca and Δ is the mass defect, both in units of MeV. SM stands for shell model and C for the estimated Coulomb displacement energy

A	Z	N	$2J$	B_{rel}^{SM}	C	Δ^{SM}
53	Ca	33	5	95.46		−25.37
54		34	0	100.10		−21.95
55		35	5	100.75		−14.52
56		36	0	104.14		−9.85
57		37	5	104.01		−1.64
58		38	0	106.30		4.11
59		39	1	104.75		13.76
60		40	0	106.94		19.64
56	Sc	35	6	117.25	7.07	−23.73
57		36	7	120.52	7.06	−18.93
58		37	10	121.51	7.05	−11.85
59		38	7	124.10	7.04	−6.37
60		39	5	124.13	7.03	1.673
61		40	7	125.74	7.02	8.13
58	Ti	36	0	139.27	14.21	−30.39
59		37	5	140.44	14.16	−23.50
60		38	0	144.15	14.12	−19.13
61		39	1	143.80	14.08	−10.71
62		40	0	146.77	14.04	−5.61
61	V	38	7	160.08	21.68	−27.77
62		39	5	161.34	21.62	−20.96
63		40	7	164.08	21.53	−15.63
63	Cr	39	1	179.33	29.04	−31.66
64		40	0	183.69	28.92	−27.94

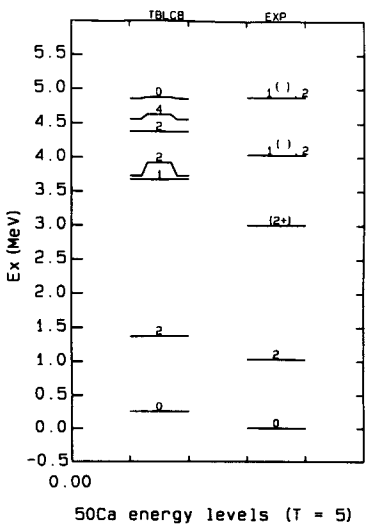

Fig. 2. Comparison of theoretical and experimental energy spectra for low-lying natural-parity levels in ^{50}Ca. The experimental spectrum (from Ref. [17]) is compared with the spectrum based on the TBLC8 interaction, with the experimental ground-state energy taken as zero. J is indicated for A even and $2J$ for A odd.

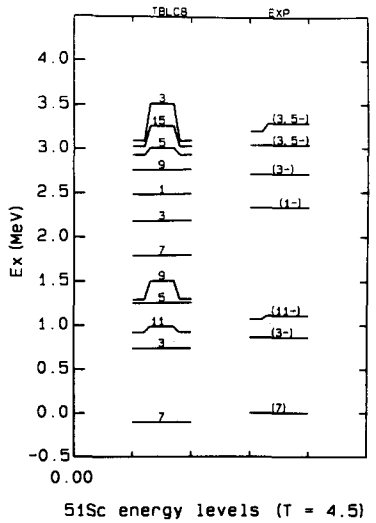

Fig. 3. Energy levels of ^{51}Sc. Conventions are the same as in Fig. 2. The experimental spectrum is from Ref. [18].

^{51}Sc: The calculation gives excitation energies of the first $\frac{3}{2}^-$ and $\frac{11}{2}^-$ states of 0.84 and 1.02 MeV, compared to the experimental values of 0.860 and 1.062 MeV, respectively. The theoretical value obtained for the first $\frac{1}{2}^-$ level of 2.59 MeV also compares favourably with the experimental value of 2.347 MeV. The tentative spin assignments and positions of the experimental energy levels appear to indicate that they generally have counterparts in the theoretical spectrum.

^{52}Ti: The calculation gives excitation energies of the first 2^+ and 4^+ states of 1.06 and

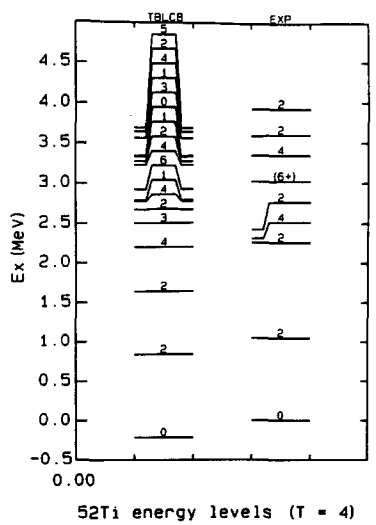

Fig. 4. Energy levels of ^{52}Ti. Conventions are the same as in Fig. 2. The experimental spectrum is from Ref. [19].

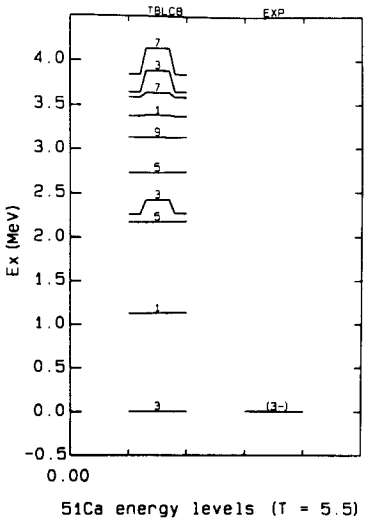

Fig. 5. Energy levels of ^{51}Ca. Conventions are the same as in Fig. 2. The experimental spectrum is from Ref. [18].

2.43 MeV, compared to the experimental values of 1.050 and 2.425 MeV, respectively. The theoretical value obtained for the first 6^+ level of 3.147 MeV also compares favourably with the experimental value of 3.028 MeV. The measured energy levels agree reasonably well on the whole with the predicted ones.

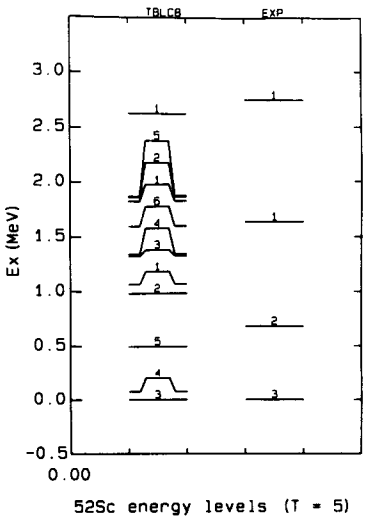

Fig. 6. Energy levels of ^{52}Sc. Conventions are the same as in Fig. 2. The experimental spectrum is from Refs. [19,14].

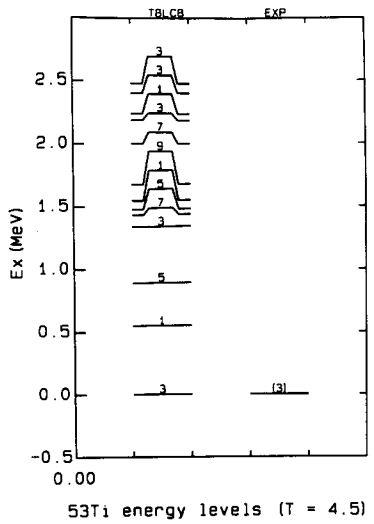

Fig. 7. Energy levels of ^{53}Ti. Conventions are the same as in Fig. 2. The experimental spectrum is from Ref. [20].

4.2. The N=31 isotones

^{51}Ca: The experimental information is very limited, and only the ground state has been assigned a tentative spin of $\frac{3}{2}$. The calculation also predicts a $\frac{3}{2}^-$ ground state. The excitation energy of the first $\frac{1}{2}^-$ state is calculated to be at 1.13 MeV.

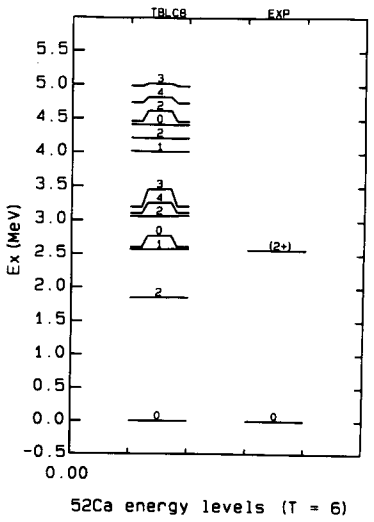

Fig. 8. Energy levels of ^{52}Ca. Conventions are the same as in Fig. 2. The experimental spectrum is from Ref. [19].

^{52}Sc: Huck et al. calculated the ^{52}Sc ground state in the model space $0f^{9}_{7/2}(1p_{3/2} \times 0f_{5/2}1p_{1/2})^3$ due to computer limitations. However, in our calculations we made use of the full $0f^{9}_{7/2}(1p_{3/2}0f_{5/2}1p_{1/2})^3 + 0f^{8}_{7/2}(1p_{3/2}0f_{5/2}1p_{1/2})^4$ model space. The calculation predicts a 3^+ ground state. The excitation energy of the first 2^+ state is calculated to be at 0.98 MeV. Experimentally a 3^+ ground state is also indicated, while the first 2^+ state is experimentally found to be at 0.68 MeV [14].

^{53}Ti: The experimental information is very limited in that only the ground state has been assigned a tentative spin value of $\frac{3}{2}$. The calculation also predicts a $\frac{3}{2}^-$ ground state. The excitation energy of the first $\frac{1}{2}^-$ state is calculated to be at 0.55 MeV.

4.3. The N=32 isotones

^{52}Ca: The calculation gives an excitation energy of the first 2^+ state of 1.85 MeV, which is higher than the typical 2^+ state energy but lower than the suggested experimental value of 2.563 MeV. This high energy signifies a partial $p_{3/2}$ subshell closure at $N = 32$. The dominant configurations in the ground-state wave function are 77% $f^{8}_{7/2}p^{4}_{3/2}$, 14% $f^{8}_{7/2}p^{2}_{3/2}f^{2}_{5/2}$ and 7% $f^{8}_{7/2}p^{2}_{3/2}p^{2}_{1/2}$. Huck et al. [14] obtained a ground-state wave function with a larger $f^{8}_{7/2}p^{4}_{3/2}$ component of 94% $f^{8}_{7/2}p^{4}_{3/2}$.

4.4. Conclusion

The shell-model calculations presented shows that the structure of the neutron-rich nuclei in the vicinity of the doubly closed ^{48}Ca nucleus, specifically the $N = 30$, 31 and 32 isotones can be adequately described by using a configuration space that incorporates 1p1h excitations from the $0f_{7/2}$ shell. This supports the finding of Huck et al. [14].

Acknowledgements

W.R. wishes to acknowledge the hospitality and support of the National Superconducting Laboratory, University of Michigan State. This work was supported in part by National Science Foundation Grant 94-03666.

References

[1] M.G. van der Merwe, W.A. Richter and B.A. Brown, Nucl. Phys. A 579 (1994) 173.
[2] M.G. van der Merwe, Ph.D. Thesis, University of Stellenbosch (1992).
[3] A. Etchegoyen, W.D.M. Rae, N.S. Godwin, W.A. Richter, C.H. Zimmerman, B.A. Brown, W.E. Ormand and J.S. Winfield, MSU-NSCL report 524 (1985).
[4] W.A. Richter, M.G. van der Merwe, R.E. Julies and B.A. Brown, Nucl. Phys. A 523 (1991) 325.
[5] H.L. Seifert, J.M. Wouters, D.J. Vieira, H. Wollnik, X.G. Zhou, X.L. Tu, Z.Y. Zhou and G.W. Butler, Z. Phys. A 349 (1994) 25.
[6] G. Audi and A.H. Wapstra, Nucl. Phys. A 565 (1993) 1.
[7] X.L. Tu, X.G. Zhou, D.J. Viera, J.M. Wouters, Z.Y. Zhou, H.L. Seifert and V.G. Lind, Z. Phys. A 337 (1990) 361.

[8] P. Möller and J.R. Nix, At. Data Nucl. Data Tables 39 (1988) 213.
[9] T. Tachibana, M. Uno, M. Yamahada and S. Yamahada, At. Data Nucl. Data Tables 39 (1988) 251.
[10] S. Liran and N. Zeldes, At. Data Nucl. Data Tables 17 (1976) 431.
[11] J. Jänecke and P.J. Masson, At. Data Nucl. Data Tables 39 (1988) 265.
[12] H. Horie and K. Ogawa, Prog. Theor. Phys. 46 (1971) 439.
[13] H. Horie and K. Ogawa, Nucl. Phys. A 216 (1973) 407.
[14] A. Huck, G. Klotz, A. Knipper, C. Miehe, C. Richard-Serre, G. Walter, A. Poves, H.L. Ravn and G. Marguier, Phys. Rev. C 31 (1985) 2226.
[15] A. Poves and A. Zuker, Phys. Reports 70 (1981) 235.
[16] C.M. Lederer and V.S. Shirley, eds., Table of isotopes (Wiley, New York, 1978).
[17] T.W. Burrows, Nucl. Data Sheets 61 (1990) 1.
[18] Zhou Chunmei, Nucl. Data Sheets 63 (1991) 229.
[19] Huo Junde, Hu Dailing, Sun Huibin, You Janming and Hu Baohua, Nucl. Data Sheets 58 (1989) 677.
[20] Huo Junde, Hu Dailing, Nucl. Data Sheets 61 (1990) 47.